1 **Title**

2 Bisbenzimide compounds inhibit replication of prototype and pandemic potential poxviruses

3

4 **Authors**

5 Jerzy Samolej[1], Diogo Correa Mendonca[2,3], Nicole Upfold[2,3], Marion McElwee[2,3], Mariann

6 Landsberger[1], Artur Yakimovich[4], Arvind H. Patel[2,3], Blair L. Strang[5*], Jason Mercer [1*]

7

8 [1]Insititute of Microbiology and Infection, University of Birmingham, Birmingham, UK

9 [2]MRC-University of Glasgow Centre for Virus Research, United Kingdom.

10 [3]CVR-CRUSH, MRC-University of Glasgow Centre for Virus Research, United Kingdom.

11 [4] Center for Advanced Systems Understanding (CASUS), Helmholtz-Zentrum Dresden-Rossendorf e.V.

12 (HZDR) Görlitz, Germany.

13 [5]Institute for Infection and Immunity, St George's, University of London, London, UK.

14

15 *Correspondence to: bstrang@sgul.ac.uk; j.p.mercer@bham.ac.uk

16

17

18 **Key words:** Vaccinia virus, antiviral, DNA replication, viral transcription, mpox

Abstract

We previously identified the bisbenzimide Hoechst 33342 (H42) as potent multi-stage inhibitor of the prototypic poxvirus, vaccinia virus (VACV) and several parapoxviruses. A recent report showed that novel bisbenzimide compounds similar in structure to H42 could prevent human cytomegalovirus replication. Here we assessed whether these compounds could also serve as poxvirus inhibitors. Using virological assays, we show that these bisbenzimide compounds inhibit VACV spread, plaque formation and the production of infectious progeny VACV with relatively low cell toxicity. Further analysis of the VACV lifecycle indicated that the effective bisbenzimide compounds had little impact on VACV early gene expression, but inhibited VACV late gene expression and truncated the formation of VACV replication sites. Additionally, we found that bisbenzimide compounds including H42 can inhibit both mpox (monkeypox) and a VACV mutant resistant to the widely used anti-poxvirus drug TPOXX (Tecovirimat). Therefore, the tested bisbenzimide compounds were inhibitors of both prototypic and pandemic potential poxviruses and could be developed for use in situations where anti-poxvirus drug resistance may occur. Additionally, these data suggest that bisbenzimide compounds may serve as broad activity antiviral compounds, targeting diverse DNA viruses such as poxviruses and betaherpesviruses.

Importance

The 2022 mpox (monkeypox) outbreak served as a stark reminder that due to the cessation of smallpox vaccination over 40 years ago, most of the human population remains susceptible to poxvirus infection. With only two antivirals approved for treatment of smallpox infection in humans, the need for additional anti-poxvirus compounds is evident. Having shown that the bisbenzimide H33342 is a potent inhibitor of poxvirus gene expression and DNA replication, here we extend these findings to include a set of novel bisbenzimide compounds that show anti-viral activity against mpox and a drug-resistant prototype poxvirus mutant. These results suggest that further development of bisbenzimides for treatment of pandemic potential poxviruses is warranted.

44 **Introduction**

45 The 2022 mpox (monkeypox) outbreak served as a potent reminder of the pandemic
46 potential of poxviruses (1). While existing smallpox vaccines (Imvanex and ACAM2000) provide good
47 protection against mpox infection (2), the cessation of smallpox vaccination has left the global
48 population susceptible to infection by many existing poxviruses for which vaccine efficacy is
49 unknown.

50 To supplement vaccination, novel drug strategies are required to treat poxvirus infection. In
51 the United States there are only two drugs approved for human treatment of smallpox: Tembexa
52 (also known as brincidofovir) and TPOXX (also known as Tecovirimat or ST-246) (3–6). In the United
53 Kingdom and European Union TPOXX is the only drug approved for the treatment of orthopoxvirus
54 infections including smallpox, mpox, vaccinia and cowpox. In 2022, TPOXX was approved for
55 treatment of mpox under the US CDCs expanded access investigational new drug protocol (CDC
56 2023). Despite its efficacy against many poxviruses including mpox (7), a single point mutation within
57 the poxviral genome was sufficient to give rise to TPOXX resistance (4). Therefore, the search for
58 additional anti-poxviral compounds is required.

59 We have shown that the bisbenzimide Hoechst 33342 (H42) is an effective inhibitor of
60 human and animal poxviruses *in vitro.* H42 was found to inhibit VACV DNA replication and late gene
61 expression of the prototype poxvirus, vaccinia virus (VACV), at low micromolar concentrations (8).
62 H42 is a fluorescent dye that binds within the minor groove of double-stranded DNA, preferentially
63 to AT-rich regions (9–13). As the anti-poxvirus efficacy of H42 correlated with its membrane
64 permeability and accessibility to the VACV DNA, our data suggested a model in which H42 blocked
65 DNA replication by coating cytoplasmic VACV DNA genomes (8).

66 A recent report by Finardi and co-workers showed that another bisbenzimide compound,
67 RO-90-7501 (2'-(4-aminophenyl)-[2,5'-bi-1H-benzimidazol]−5-amine) (referred to here as R90) and
68 several of its analogues produced by MRC-Technology (MRT, now LifeArc), could inhibit replication

69 of human cytomegalovirus (HCMV). This was likely to occur by binding to the HCMV DNA genome
70 and inhibiting production of HCMV capsids containing genomes (14). These compounds included
71 MRT00210423, MRT00210424, MRT00210425, MRT00210426 and MRT00210427 (14) (referred to
72 here as M23, M24, M25, M26, and M27). Given the potential broad-spectrum antiviral activity of
73 this extended class of bisbenzimide compounds against viruses with DNA genomes, we set out to
74 determine if R90 or the MRT compounds were effective inhibitors of both prototype and pandemic
75 potential poxvirus replication.

76

77 **Results**

78 **MRT compounds M23-M26 display anti-poxvirus activity.** R90 and the MRT compounds are
79 structurally similar to H42, with differences in the terminal groups of the compounds and/or
80 substitution of methyl groups for amine groups (Fig. 1A). In previous studies, the compounds R90,
81 M23, M24 and M25 which retained DNA binding activity inhibited HCMV replication (14). It was
82 noted that M23 was a more effective inhibitor of HCMV replication than R90, which may be due to
83 its greater ability to interact with DNA (14). M26 and M27 were ineffective inhibitors of HCMV
84 replication, likely due to their inability to interact with DNA (14).

85 To investigate their potential as anti-poxvirus agents we first tested the ability of R90 and
86 the MRT compounds to block VACV cell-to-cell spread. During infection poxviruses produce two
87 forms of infectious particles: mature virions (MVs) and extracellular virions (EVs). MVs are more
88 abundant and mediate host-to-host transmission, while EVs contribute to intra-host and cell-to-cell
89 virus spread (15). The VACV replication cycle is efficient, newly assembled EVs are released by 8 hpi
90 and intracellular replication is complete within 24 h (16). With this mind HeLa cells were infected
91 with VACV L-EGFP, a VACV recombinant expressing EGFP from a late viral promoter, at MOI 0.1 to
92 obtain <30% primary infection of the monolayer. To allow sufficient time for virus cell-to-cell spread
93 infection was allowed to proceed for 24 h in the absence or presence of R90 or the MRT compounds

94 at increasing concentrations. H42 and TPOXX, a tricyclononene carboxamide that inhibits the
95 production of EVs, were included as controls (4). At 24 hpi samples were analysed by flow cytometry
96 for the number of EGFP expressing cells (Fig. 1B; black lines).

97 As expected, TPOXX and H42 controls prevented virus spread at low to sub-micromolar
98 concentrations. They lowered the percentage of EGFP expressing cells by 70% and 80% respectively
99 at concentrations as low as 0.4 µM. At low micromolar concentrations R90 showed limited activity,
100 only blocking VACV spread by 20% at 40 µM. M23, M24 and M25 showed concentration dependent
101 inhibition of VACV spread. While M23 inhibitory activity plateaued between 10 µM and 40 µM, M24
102 and M25 completely blocked infection at 40 µM. M26 and M27, which potentially lack DNA binding
103 activity (14) had limited or no obvious anti-VACV activity. M26 displayed modest dose-dependent
104 inhibition of VACV spread at higher concentrations (20-40 µM) while M27 showed no anti-VACV
105 activity.

106 To ensure the observed anti-viral effects were not due to cellular cytotoxicity caused by the
107 compounds, we measured uninfected cell viability in the presence of each by assaying the ability of
108 cells to metabolise the salt WST-1. Consistent with previous reports, R90 and the MRT compounds
109 had no impact on cell viability at the concentrations used, while H42 displayed toxicity at higher
110 concentrations outside of the effective range of VACV inhibition (Fig. 1B; red lines) (8, 14).

111 The half maximal inhibitory concentration (IC50) and half maximal cell cytotoxicity
112 concentration (CC50) measurements indicate that H42 and the MRT compounds M23-M25 display
113 anti-poxvirus activity, without obvious cellular cytotoxicity (Fig. 1). Compounds R90, M26 and M27
114 displayed poor or no anti-VACV activity, which may be due to factors that include their poor ability
115 to associate with DNA.

116 **MRT compounds M23, M24 and M25 reduce VACV yield and block plaque formation.**
117 Having determined that R90 and the MRT compounds have varying effects on VACV spread, we next
118 assessed their ability to prevent virus production. The effective concentration against VACV for each

119 compound was determined from the cell-to-cell spread assays shown in Figure 1. These compound
120 concentrations were used in subsequent experiments, including virus production assays (see Figures
121 and Figure Legends). HeLa cells were infected with WT VACV at an MOI of 1 in the presence of R90,
122 M23, M24, M25, M26 or M27. Infection in the presence of H42 served as a control for inhibition of
123 virus production. At 24 hpi cells were harvested and the infectious virus yield determined by plaque
124 assay (Fig. 2A). Similar to the results of the cell-to-cell spread assay (Fig. 1), M27 was ineffective and
125 did not impact VACV yield at 24 h while R90 and M26 showed only a modest (≤1 log) reduction in
126 viral yield. M23, M24 and M25 all reduced virus yield by 3-3.5 logs, confirming the inhibitory effects
127 of these three MRT compounds.

128 We next assayed plaque formation in the presence of the effective compounds. Focusing on
129 M23, M24 and M25 we infected confluent human retinal pigment epithelia cells (A-RPE-19s) with
130 WT VACV in the presence of the MRT compounds, DMSO, TPOXX or H42. At 48 hpi, monolayers were
131 stained and assessed for VACV plaque formation (Fig. 2B). M23, M24 and M25 were found to
132 effectively inhibit VACV plaque formation. These results indicate that M23, M24, and M25 inhibit
133 VACV production and that they maintain anti-poxvirus activity for at least 48 hours. This is consistent
134 with our finding that H42 retained anti-poxvirus activity for at least 72 h (8).

135 **M23, M24, and M25 inhibit VACV gene expression.** We have shown that H42 inhibits
136 poxvirus gene expression (8). To ascertain if the MRT compounds act in a similar fashion we infected
137 HeLa cells in the presence of M23, M24 or M25 at an MOI of 20 with VACV E-EGFP or VACV L-EGFP
138 (recombinant VACVs expressing EGFP from an early or late viral promoter, respectively). As VACV
139 early gene expression (EGE) occurs before DNA replication and late gene expression (LGE) after DNA
140 replication, we included cycloheximide (CHX) and Cytosine Arabinoside (AraC) controls which inhibit
141 EGE and LGE, respectively. A TPOXX control was also included as a late-stage block that does not
142 affect viral gene expression (8). Cells were harvested at 8 hpi and the number of E-EGFP and L-EGFP
143 expressing cells were quantified by flow cytometry (Fig. 3A). Compared to CHX, H42, M23, M24 and

144 M25 had very modest effects on EGE. Conversely, all bisbenzimide compounds effectively
145 diminished LGE to the levels seen in the presence of AraC. As expected TPOXX had no effect on
146 either EGE or LGE.

147 **M23, M24 and M25 reduce the size of VACV replication sites.** To corroborate the gene
148 expression results we infected cells with VACV EGFP-A5 (a VACV recombinant that expresses an
149 EGFP-tagged version of the VACV late core protein A5) in the presence of the various compounds. At
150 24 hpi cells were fixed and immunostained for the early VACV protein I3, which is found on uncoated
151 genomes and within VACV replication sites (Fig. 3B). As expected, I3- and A5 co-localised in large
152 replication sites in the presence of either DMSO or TPOXX. In the presence of CHX, which prevents
153 VACV genome uncoating (17), stabilized A5-positive virus cores, but no I3- or A5-positive replication
154 sites were observed. In the presence of AraC, I3-positive uncoated genomes and A5-positive
155 incoming cores were observed, but no VACV replication sites were seen. In the presence of
156 bisbenzimide compounds, small I3-positive, A5-negative replication sites were observed. The
157 replication sites were similar to those seen in the presence of H42, being far smaller and "more
158 compact" than those seen in infected, DMSO-treated controls (8). A5 was not robustly expressed in
159 the presence of any bisbenzimide compound, therefore, no replication sites in which I3 and A5 co-
160 localised were observed. Overall, this data demonstrated that all bisbenzimide compounds inhibit
161 LGE (Fig. 3A), which in turn blocked the development of VACV replication sites (Fig. 4B).

162 **Bisbenzimides H42, M23, M24 and M25 inhibit mpox infection.** We have shown that H42 is
163 effective against orthopox- and parapox- viruses, suggesting that the bisbenzimides display broad
164 anti-poxviral activity (8). Given the recent worldwide mpox outbreak we wanted to assess if H42 and
165 MRT compounds could inhibit mpox. Human foetal foreskin fibroblast (Hft) cells were infected with a
166 WT mpox strain, isolated during the recent pandemic, in presence of H42 or the MRT compounds at
167 various concentrations. At 48 hpi cells were assessed, in parallel, for cytopathic effect (CPE) and cell
168 cytotoxicity (Fig. 4).

169 We employed TPOXX as a control for inhibition of mpox spread (4). As expected, TPOXX
170 displayed potent anti-mpox activity with no apparent toxicity (Fig. 4). H42 and the three MRT
171 compounds were also found to be effective mpox inhibitors with IC50s of 0.075 µM for H42, 4.0 µM
172 for M23, 1.9 µM for M24 and 6.1 µM for M25. H42, M23 and M24 were most effective, completely
173 blocking mpox CPE at 0.22 µM, 13.3 µM, and 4.4 µM, respectively (Fig 4; blue lines). M25, at its most
174 effective concentration (4.4 µM), reduced CPE to <40%. At these concentrations, H42 caused 50%,
175 M23 48%, M24 27% and M25 21% cell cytotoxicity, with CC50s of 0.19 µM for H42, 24 µM for M23,
176 15 µM for M24 and 18 µM for M25. While the Hft cells used for the mpox assay appear to be more
177 sensitive to the compounds than HeLa, A-RPE-19 and BSC cells, overall, these data indicated that
178 bisbenzimides were effective inhibitors of mpox replication.

179 **Bisbenzimides effectively inhibit TPOXX resistant VACV.** TPOXX was approved for treatment of
180 mpox under the US CDCs expanded access investigational new drug protocol in 2022. It remains the
181 only drug approved for the treatment of both smallpox and mpox. TPOXX targets the viral envelope
182 wrapping protein F13, which is conserved in all poxviruses. Single point mutations in the gene
183 encoding F13 are known to confer TPOXX resistance to poxviruses *in vitro* and *in vivo* (18, 19).

184 Thus, we were curious to see if the bisbenzimides could inhibit spread of a VACV that is
185 partially resistant to TPOXX. For this, we used a VACV expressing the F13 mutant (G277C), which has
186 been described to lower the antiviral efficacy of TPOXX both *in vitro* and *in vivo* (4, 20). To assure
187 that any phenotypes observed were due to the presence of the G277C mutation and not any other
188 unknown mutations, we generated a control virus - RevG277C- in which the G277C mutant virus was
189 repaired. To examine the effect on virus spread, HeLa cells were infected at a low MOI (0.01) with
190 WT, G277C or RevG277C. Infections were performed in the presence of DMSO, TPOXX, H42 or M23.
191 Cells were harvested at 24 hpi and the virus production quantified by plaque assay (Fig. 5A). TPOXX
192 effectively lowered WT and RevG277C control virus production by >95% compared to the DMSO
193 control. The G277C mutant virus, as expected, showed some resistance to TPOXX (70% reduction).

194 Both H42 and M23 effectively blocked production of VACV WT, G277C mutant, and RevG277C
195 control viruses, in each case decreasing virus yield by >3.5 log.

196 To assess the effect of the compounds on plaque formation, A-RPE-19 cells were infected
197 with VACV WT, G277C or RevG277C in the presences of DMSO, TPOXX [0.4µM], H42 [0.4µM] or M23
198 [10µM] (Fig.5B). As expected, in the presence of DMSO all viruses formed plaques. Both WT and
199 VACV RevG277C control virus were sensitive to TPOXX, while the G277C mutant virus was resistant
200 (albeit, forming somewhat smaller plaques). Consistent with the 24 h yield results (Fig. 5A), H42 and
201 M23 both completely abrogated VACV WT, G277C and RevG277C virus plaque formation.

202 To confirm that the mechanism of H42 and M23 inhibition remained the same, HeLa cells
203 were infected with G277C or the RevG277C control virus in the presence of DMSO, H42 or M23. At
204 24 hpi cells were fixed and viral replication sites visualized by immunostaining for I3 (Fig. 5C). In the
205 presence of DMSO, infection with both VACV viruses produced large I3-positive replication sites. In
206 the presence of H42 or M23 I3-postive replication sites were reduced in number and size (Fig. 5C).
207 Collectively, these results indicated that H42 and M23 are effective inhibitors of a TPOXX-resistant
208 mutant VACV.

209

210 **Discussion**

211 We have previously shown that bisbenzimides are potent inhibitors of poxvirus infection (8). We
212 found that these compounds, which preferentially bind the minor groove of double-stranded DNA,
213 inhibit infection by blocking DNA replication and post-replicative gene transcription. The
214 bisbenzimide H42 was found to inhibit a range of human and animal poxviruses but was ineffective
215 against several other DNA and RNA viruses, including herpes simplex virus-1 (HSV-1) and influenza A.

216 Here, we tested a series of novel bisbenzimide analogues, with reported activity against HCMV
217 (14), against VACV and mpox. Three of these compounds M23, M24 and M25 proved to be effective

218 inhibitors of prototype (VACV) and pandemic potential (mpox) poxviruses with low cytotoxicity. We
219 show that, like H42 (8), these compounds block poxvirus replication and subsequent LGE.

220 Poxviruses with varied genomic AT content, ranging from VACV (67% AT) to squirrel pox SQPV
221 (33% AT) (21) showed similar sensitivity to H42 [1]. Thus, we concluded that the inhibitory efficacy of
222 the bisbenzimides did not correlate with their preferential binding to adenosine-threonine (AT)-rich
223 regions of DNA; but with the cytoplasmic accessibility of replicating poxvirus genomes and the
224 lipophilicity of the bisbenzimide compounds, which largely dictates their binding to double-stranded
225 DNA via hydrophobic interactions with adenosine/threonine-rich regions (9, 22, 23). Consistent with
226 this model, in the presence of the MRT compounds VACV DNA replication sites were small and
227 condensed, and the IC50s of R90, H42, M23, M24, M25 in HeLa cells largely correlated with their
228 predicted lipophilicity (LogP): H42>M23>M24=M25>R90 (Fig. 1A). This of course does not preclude
229 other properties of these compounds that might affect their efficacy, such as membrane
230 permeability and toxicity.

231 We further show that H42, M23, M24, and M25 were all effective at blocking mpox infection.
232 When assaying mpox replication, TPOXX showed high efficacy and low cytotoxicity compared to the
233 MRT compounds. Despite its *in vitro* potency, as TPOXX targets a viral protein it is subject to
234 mutational resistance (4, 24). During the 2022 mpox pandemic, TPOXX resistant mutants were in fact
235 isolated from mpox patients undergoing TPOXX treatment (18, 19). We found that H42 and the
236 MRTs were still effective against a virus that shows resistance to TPOXX. This is not surprising as the
237 bisbenzimides target a different stage in VACV replication than TPOXX (late gene expression and
238 virus assembly/release, respectively) and interact with different factors required for VACV
239 replication (protein F13 and the VACV DNA genome, respectively). As yet we have been unable to
240 isolate a H42-resistant mutant virus in more than 20 passages of VACV *in vitro* (data not shown)
241 (Similar observations have been made passaging HCMV in the presence of a bisbenzimide (RO) (14).

[1] (8)

242 Thus, the bisbenzimide compounds do not appear to be subject to the development of VACV
243 resistance. This suggests that TPOXX/bisbenzimide co-inhibition studies could be further explored
244 for additive or synergistic effects against poxvirus infection.

245 It is interesting to compare the mechanisms of action of bisbenzimide compounds on poxviruses
246 and HCMV. At low concentrations, bisbenzimides inhibit VACV gene expression but prevent the
247 formation of HCMV genome-containing capsids (14). While at higher concentrations both VACV and
248 HCMV genome replication is blocked (8, 14). Given that the anti-viral effects correlate with low
249 concentration bisbenzimide treatment it may be worth examining the relationship between HCMV
250 gene expression and genome packaging.

251 Collectively, this work supports further exploration of bisbenzimides as anti-viral agents. This is
252 supported by the long-standing observations that some bisbenzimide compounds have no obvious
253 adverse effects in mice and have been used with no serious adverse effects in human clinical trials
254 (25). Using the compounds tested here as a platform to generate modified bisbenzimide analogues,
255 in the future we hope to identify new bisbenzimides with increased potency against poxviruses and
256 perhaps other DNA virus families.

257

258 **Materials and Methods**

259 ***Cells, viruses, and compounds***

260 HeLa (ATCC), BSC-40, A-RPE-19 (kind gift from Frickel lab, UoB), Vero E6, and Primary Human foetal
261 foreskin fibroblasts immortalized by retrovirus transduction to express the catalytic subunit of
262 human telomerase (Hft) (26) were maintained at 37.0 °C and 5.0% CO_2 in Dulbecco's modified
263 Eagle's medium (DMEM; Gibco, Life Technologies) with the addition of 10% foetal bovine serum
264 (FBS; Sigma), and 1% penicillin-streptomycin (Pen-Strep; Sigma).

265 Vaccinia virus strain Western Reserve (VACV) was used throughout. VACVs used were either wild
266 type (WT) or transgenic, containing EGFP under early VACV gene promoter (VACV E-EGFP), late
267 VACV gene promoter EGFP (VACV L-EGFP), or A5-tagged EGFP inserted into the endogenous A5 locus
268 (VACV EGFP-A5). WT, E-EGFP (27), L-EGFP (27) and EGFP-A5 (28) were previously published. All VACV
269 mature virions (MVs) were purified from BSC40 cytoplasmic lysates by being pelleted through a 36%
270 sucrose cushion for 90 min at 18,000 × g. The virus pellet was resuspended in 1 mM Tris (pH 9.0).
271 The titre (PFU per millilitre) was determined in BSC40 cells as previously described. MPox virus
272 (accession number: ON808413; strain designation MPXV CVR-S1) was isolated from a clinical sample
273 in Glasgow in 2022 (29). Vero cells were used to propagate mpox. HFt cells were used in antiviral
274 activity and toxicity assays.

275 Cycloheximide (CHX; Sigma), cytosine arabinoside (AraC, Sigma), and TPOXX (generously provided by
276 Dennis Hruby and Douglas Grosenbach , SIGA Technologies, Inc.) were diluted in DMSO and used as
277 indicated in the text and figures and figure legends. Bisbenzimides Hoechst 33342 (H42, Sigma), RO-
278 90-7501 (R90; Sigma); MRT00210423, MRT00210424, MRT00210425, MRT00210426, MRT00210427
279 (all generously provided by Andy Merritt, LifeArc (formerly MRC Technology)) were dissolved in
280 DMSO and used at concentrations indicated in the text and figures and figure legends. DMSO was
281 used as a drug carrier control at the same volume as drug or compound diluted in DMSO.

282 **Bisbenzimide predicted lipophilicity**

283

284 To determine the non-ionic consensus partitioning coefficient (LogP) of all structures we
285 used AxonChem Marvin cheminformatics suite. Calculations for all structures assumed Cl-
286 and Na+ K+ concentrations of 0.1 mol/dm3 each. Tautomerization or resonance were not
287 considered.

288

289 ***Flow cytometry***

290 HeLa cells in 96 well plates were infected with VACV L-EGFP at MOI 0.5 for 24 h (Spread Assay); or
291 VACV E-EGFP or L-EGFP at MOI 20 for 8h (EGE or LGE assay). After 30 min at room temperature (RT)
292 the inoculant was replaced with DMEM containing compounds at indicated concentrations. For
293 Spread Assay: TPOXX, H42, AraC: 40-4-0.4-0.04-0.004-0.0004 µM; R90, M23-27: 40-20-10-5-2.5-1.25
294 µM. For EGE or LGE, effective concentration (EC) with acceptable cytotoxicity derived from the
295 Spread Assay was used. (Effective concentration was the compound concentration where at least
296 90% of cells in an infected well were ***not*** expressing GFP.) After incubation at 37 °C wells were
297 aspirated and cells detached with trypsin, followed by addition of 5% BSA in PBS and fixation with
298 9% formaldehyde in PBS (for a final 3% FA concentration). The percentage of green fluorescent cells
299 out of all cells was then counted using a Guava® easyCyte™ flow cytometer. Gating was done using
300 "live cells" gate first, and then a "<99% of uninfected cells are below threshold" gate. The results – %
301 of cells expressing GFP – were then normalised to infected, DMSO-treated controls (DMSO = 1).
302 IC50/CC50 concentrations were determined in GraphPad Prism using a four-parameter logistic
303 nonlinear regression model (Inhibitor) vs response – four parameters).

304 ***Cytotoxicity***

305 Cytotoxicity was assessed using Abcam's Quick Cell Proliferation Assay Kit II (WST-1), following
306 manufacturers' instructions. Briefly, HeLa cells in 96-well plates were incubated for 24 h at 37 °C in
307 the compound concentrations mirroring those concentrations used in the flow cytometry Spread
308 Assay. WST solution was then added to each well and incubated for 3 h, followed by absorbance
309 measurement at 460nm, corrected by subtracting absorbance in wells without cells but with media.
310 Values were then normalized to cells incubated without any compounds.

311 ***Virus yield and spread assays***

312 HeLa cell monolayers in 6-well plates were infected with VACV WT at MOI 1 (24 h yield) or MOI 0.01
313 (24 h spread) in presence of specified compound. At 24 hpi, cells were collected and centrifuged,
314 and the pellet was resuspended in 100 µl 1 mM Tris (pH 9.0). Cells were then freeze-thawed three

315 times to lyse the cells, and the lysate solution was serially diluted to determine the PFU per millilitre
316 by plaque assay on BSC40 cell monolayers.

317 ***Plaque inhibition assays***

318 A-RPE-19 cells grown in 12-wells were infected with 200 pfu of VACV WT, G277C, or G277C-rev in
319 the presence of specified compound at 37 °C. 48 hpi cells were fixed and stained with 0.1% crystal
320 violet in 4% formaldehyde. Plate images were digitally captured using a desktop scanner (Cannon).

321 ***Immunofluorescence microscopy***

322 HeLa were cells seeded on CellView slides (Greiner Bio-One). They were infected with VACV EGFP-A5
323 for 30 min at RT. The inoculant was then replaced with indicated compounds in the text, figures and
324 figure legends. After 20 h at 37 °C cells were washed and fixed with 4% EM grade FA in PBS. They
325 were permeabilized and blocked simultaneously in 0.5% Triton-X 1000 in 5% BSA in PBS. Anti-I3
326 antibody (generously provided by Jakomine Krijnse Locker; Institute Pasteur) was used at 1:1,000. All
327 secondary antibodies (goat anti-mouse-AF488 and goat anti-rabbit-AF647; Invitrogen) were used at
328 1:1,000. Primary I3 antibody was added for 60 min at RT, followed by a wash and 60 min RT staining
329 with secondary antibody and DAPI. Images were captured using a 100x oil immersion objective (NA
330 1.45) on a VT-iSIM microscope (Visitech; Nikon Eclipse TI), using 488 nm and 640 nm laser
331 frequencies for excitation.

332 ***Mpox antiviral activity and toxicity assays.***

333 HFt cells were seeded in 96-well plates (Costar) at a density of $1x10^4$ cells per well and incubated for
334 24 hours. Three hours prior to infection, the cells were incubated with three-fold serial dilutions of
335 each compound prepared in infection medium (DMEM containing 2% FBS). For mpox antiviral
336 assays, the plates were transferred to a CL3 facility before each well was infected with an equal
337 volume of infection medium containing mpox virus at an MOI of 0.1 ($1.4x10^3$ plaque forming units
338 (PFU)) per well. Following incubation for 48 hours, cells were fixed in 8% formaldehyde in PBS and

339 stained with Coomassie Blue. The dried plates were scanned using a Pherastar SFX plate reader
340 (BMG) at an optical density of 595 nm to quantitate the level of cytopathic effect (CPE). For toxicity
341 assays, an equal volume of infection medium without virus was added to each well. Following 48
342 hours, 10 µl of resazurin (Sigma R7017) prepared at a concentration of 0.5 mM in PBS was added to
343 each well. After a 2h incubation period, resofurin was quantified by measuring fluorescence
344 intensity (Ex530/Em560) using a Varioskan LUX microplate reader (Thermo Scientific). Percentage
345 virus replication was calculated by normalising well clearance to infected and uninfected DMSO
346 controls, while percentage cell viability was determined by normalising values to untreated cells and
347 our high toxicity control (50% DMSO). IC50/CC50 concentrations were determined in GraphPad
348 Prism using a four-parameter logistic nonlinear regression model (Inhibitor) vs normalized response
349 – four parameters).

350

351 **References**

352 1. Thornhill JP, Barkati S, Walmsley S, Rockstroh J, Antinori A, Harrison LB, Palich R, Nori A, Reeves
353 I, Habibi MS, Apea V, Boesecke C, Vandekerckhove L, Yakubovsky M, Sendagorta E, Blanco JL,
354 Florence E, Moschese D, Maltez FM, Goorhuis A, Pourcher V, Migaud P, Noe S, Pintado C,
355 Maggi F, Hansen A-BE, Hoffmann C, Lezama JI, Mussini C, Cattelan A, Makofane K, Tan D, Nozza
356 S, Nemeth J, Klein MB, Orkin CM, SHARE-net Clinical Group. 2022. Monkeypox Virus Infection
357 in Humans across 16 Countries - April-June 2022. N Engl J Med 387:679–691.

358 2. Bertran M, Andrews N, Davison C, Dugbazah B, Boateng J, Lunt R, Hardstaff J, Green M,
359 Blomquist P, Turner C, Mohammed H, Cordery R, Mandal S, Campbell C, Ladhani SN, Ramsay
360 M, Amirthalingam G, Bernal JL. 2023. Effectiveness of one dose of MVA-BN smallpox vaccine
361 against mpox in England using the case-coverage method: an observational study. Lancet Infect
362 Dis 23:828–835.

363 3. Olson VA, Smith SK, Foster S, Li Y, Lanier ER, Gates I, Trost LC, Damon IK. 2014. In Vitro Efficacy
364 of Brincidofovir against Variola Virus. Antimicrob Agents Chemother 58:5570–5571.

365 4. Yang G, Pevear DC, Davies MH, Collett MS, Bailey T, Rippen S, Barone L, Burns C, Rhodes G,
366 Tohan S, Huggins JW, Baker RO, Buller RLM, Touchette E, Waller K, Schriewer J, Neyts J,
367 DeClercq E, Jones K, Hruby D, Jordan R. 2005. An Orally Bioavailable Antipoxvirus Compound
368 (ST-246) Inhibits Extracellular Virus Formation and Protects Mice from Lethal Orthopoxvirus
369 Challenge. J Virol 79:13139–13149.

370 5. Blasco R, Moss B. 1991. Extracellular vaccinia virus formation and cell-to-cell virus transmission
371 are prevented by deletion of the gene encoding the 37,000-Dalton outer envelope protein. J
372 Virol 65:5910–5920.

373 6. Chinsangaram J, Honeychurch KM, Tyavanagimatt SR, Leeds JM, Bolken TC, Jones KF, Jordan R,
374 Marbury T, Ruckle J, Mee-Lee D, Ross E, Lichtenstein I, Pickens M, Corrado M, Clarke JM, Frimm
375 AM, Hruby DE. 2012. Safety and pharmacokinetics of the anti-orthopoxvirus compound ST-246
376 following a single daily oral dose for 14 days in human volunteers. Antimicrob Agents
377 Chemother 56:4900–4905.

378 7. Jordan R, Goff A, Frimm A, Corrado ML, Hensley LE, Byrd CM, Mucker E, Shamblin J, Bolken TC,
379 Wlazlowski C, Johnson W, Chapman J, Twenhafel N, Tyavanagimatt S, Amantana A,
380 Chinsangaram J, Hruby DE, Huggins J. 2009. ST-246 Antiviral Efficacy in a Nonhuman Primate
381 Monkeypox Model: Determination of the Minimal Effective Dose and Human Dose
382 Justification. Antimicrobial Agents and Chemotherapy 53:1817–1822.

383 8. Yakimovich A, Huttunen M, Zehnder B, Coulter LJ, Gould V, Schneider C, Kopf M, McInnes CJ,
384 Greber UF, Mercer J. 2017. Inhibition of Poxvirus Gene Expression and Genome Replication by
385 Bisbenzimide Derivatives. J Virol 91:e00838-17.

386 9. Fornander LH, Wu L, Billeter M, Lincoln P, Nordén B. 2013. Minor-groove binding drugs: where
387 is the second Hoechst 33258 molecule? J Phys Chem B 117:5820–5830.

388 10. Han F, Taulier N, Chalikian TV. 2005. Association of the minor groove binding drug Hoechst
389 33258 with d(CGCGAATTCGCG)2: volumetric, calorimetric, and spectroscopic characterizations.
390 Biochemistry 44:9785–9794.

391 11. Smith PJ, Lacy M, Debenham PG, Watson JV. 1988. A mammalian cell mutant with enhanced
392 capacity to dissociate a bis-benzimidazole dye-DNA complex. Carcinogenesis 9:485–490.

393 12. Latt SA, Stetten G. 1976. Spectral studies on 33258 Hoechst and related bisbenzimidazole dyes
394 useful for fluorescent detection of deoxyribonucleic acid synthesis. J Histochem Cytochem
395 24:24–33.

396 13. Comings DE, Avelino E. 1975. Mechanisms of chromosome banding. VII. Interaction of
397 methylene blue with DNA and chromatin. Chromosoma 51:365–379.

398 14. Falci Finardi N, Kim H, Hernandez LZ, Russell MRG, Ho CM-K, Sreenu VB, Wenham HA, Merritt
399 A, Strang BL. 2021. Identification and characterization of bisbenzimide compounds that inhibit
400 human cytomegalovirus replication. J Gen Virol 102:001702.

401 15. Stiefel P, Schmidt FI, Dörig P, Behr P, Zambelli T, Vorholt JA, Mercer J. 2012. Cooperative
402 vaccinia infection demonstrated at the single-cell level using FluidFM. Nano Lett 12:4219–
403 4227.

404 16. Youngner JS, Furness G. 1959. One-step growth curves for vaccinia virus in cultures of monkey
405 kidney cells. Virology.

406 17. Mercer J, Snijder B, Sacher R, Burkard C, Bleck CKE, Stahlberg H, Pelkmans L, Helenius A. 2012.
407 RNAi screening reveals proteasome- and Cullin3-dependent stages in vaccinia virus infection.
408 Cell Rep 2:1036–1047.

409 18. Smith TG, Gigante CM, Wynn NT, Matheny A, Davidson W, Yang Y, Condori RE, O'Connell K,
410 Kovar L, Williams TL, Yu YC, Petersen BW, Baird N, Lowe D, Li Y, Satheshkumar PS, Hutson CL.
411 2023. Resistance to anti-orthopoxviral drug tecovirimat (TPOXX®) during the 2022 mpox
412 outbreak in the US. medRxiv https://doi.org/10.1101/2023.05.16.23289856.

413 19. Garrigues JM, Hemarajata P, Karan A, Shah NK, Alarcón J, Marutani AN, Finn L, Smith TG,
414 Gigante CM, Davidson W, Wynn NT, Hutson CL, Kim M, Terashita D, Balter SE, Green NM. 2023.
415 Identification of Tecovirimat Resistance-Associated Mutations in Human Monkeypox Virus - Los
416 Angeles County. Antimicrob Agents Chemother 67:e0056823.

417 20. Duraffour S, Lorenzo MM, Zöller G, Topalis D, Grosenbach D, Hruby DE, Andrei G, Blasco R,
418 Meyer H, Snoeck R. 2015. ST-246 is a key antiviral to inhibit the viral F13L phospholipase, one
419 of the essential proteins for orthopoxvirus wrapping. J Antimicrob Chemother 70:1367–1380.

420 21. Hatcher EL, Wang C, Lefkowitz EJ. 2015. Genome variability and gene content in
421 chordopoxviruses: dependence on microsatellites. Viruses 7:2126–2146.

422 22. Chang DK, Cheng SF. 1996. On the importance of van der Waals interaction in the groove
423 binding of DNA with ligands: restrained molecular dynamics study. Int J Biol Macromol 19:279–
424 285.

425 23. Sauers RonaldR. 1995. An analysis of van der Waals attractive forces in DNA-minor groove
426 binding. Bioorganic & Medicinal Chemistry Letters 5:2573–2576.

427 24. Smee DF, Sidwell RW, Kefauver D, Bray M, Huggins JW. 2002. Characterization of wild-type and
428 cidofovir-resistant strains of camelpox, cowpox, monkeypox, and vaccinia viruses. Antimicrob
429 Agents Chemother 46:1329–1335.

430 25. Patel SR, Kvols LK, Rubin J, O'Connell MJ, Edmonson JH, Ames MM, Kovach JS. 1991. Phase I-II
431 study of pibenzimol hydrochloride (NSC 322921) in advanced pancreatic carcinoma. Invest New
432 Drugs 9:53–57.

433 26. Conn KL, Wasson P, McFarlane S, Tong L, Brown JR, Grant KG, Domingues P, Boutell C. 2016.
434 Novel Role for Protein Inhibitor of Activated STAT 4 (PIAS4) in the Restriction of Herpes Simplex
435 Virus 1 by the Cellular Intrinsic Antiviral Immune Response. J Virol 90:4807–4826.

436 27. Schmidt FI, Bleck CKE, Reh L, Novy K, Wollscheid B, Helenius A, Stahlberg H, Mercer J. 2013.
437 Vaccinia virus entry is followed by core activation and proteasome-mediated release of the
438 immunomodulatory effector VH1 from lateral bodies. Cell Rep 4:464–476.

439 28. Schmidt FI, Bleck CKE, Helenius A, Mercer J. 2011. Vaccinia extracellular virions enter cells by
440 macropinocytosis and acid-activated membrane rupture. EMBO J 30:3647–3661.

441 29. Davis C, Epifano I, Dee K, McFarlane S, Wojtus JK, Brennan B, Gu Q, Vattipally SB, Nomikou K,
442 Tong L, Orr L, Filipe ADS, Ho A, Thomson EC, Boutell C. 2023. Temperature elevation synergises
443 with and enhances the type-I IFN-mediated restriction of MPXV. bioRxiv
444 https://doi.org/10.1101/2023.09.29.560106.

445

446

447 **Author Contributions**

448 JS: Data Analysis and Curation, Methodology, Supervision, Writing-Original Draft Preparation, Writing-
449 Review and Editing. DCM: Conceptualization, Methodology, Investigation, Data Analysis and Curation
450 and Writing-Review and Editing. NU: Conceptualization, Methodology, Investigation, Data Analysis
451 and Curation and Writing-Review and Editing. MMcE: Investigation. ML: Investigation. AY:
452 Investigation, Writing-Review and Editing. AHP: Supervision, Writing-Review and Editing and Funding.
453 BLS: Conceptualization, Methodology, Writing-Original Draft Preparation, Writing-Review and Editing.
454 JPM: Conceptualization, Methodology, Writing-Original Draft Preparation, Writing-Review and
455 Editing, Supervision, Project Administration and Funding.

456 **Conflict of Interest**

457 The authors declare no conflicts of interest.

458 **Acknowledgments**

459 We thank Andy Merritt (LifeArc) for the generous provision of reagents and his support of the
460 project throughout. We thank Dennis Hruby and Douglas Grosenbach (SIGA Technologies, Inc.) for
461 providing TPOXX.

462 **Funding**

463 BLS was supported by St George's, University of London. JM was supported by the Medical Research
464 Council [MC_PC_19029] and the BBSRC-funded mpox rapid response grant BB/X011607/1. The mpox
465 virus work was carried out by CRUSH: Antiviral Drug Screening and Resistance Hub at the MRC-
466 University of Glasgow Centre for Virus Research (CVR). Funding for this research was supported by
467 the BBSRC-funded mpox rapid response grant BB/X011607/1, LifeArc COVID-19 award, and the MRC
468 core award MC_UU_00034/9 (AHP). This work was partially funded by the Center for Advanced
469 Systems Understanding (CASUS) which is financed by Germany's Federal Ministry of Education and

Research (BMBF) and by the Saxon Ministry for Science, Culture, and Tourism (SMWK) with tax funds on the basis of the budget approved by the Saxon State Parliament (AY).

473 **Figure Legends**

474 **Fig 1. MRT compounds inhibit cell-to-cell spread of VACV.**

475 A) Structures of Bisbenzemides and MRT compounds. H42 (Hoechst 33342), R90 (RO-90-7501), M23
476 (MRT00210423), M24 (MRT00210424), M25 (MRT00210425), M26 (MRT00210426) and M27
477 (MRT00210427). Respective partitioning coefficient (LogP) and chemical abstract number (CAS)
478 where applicable are provided below. B) HeLa cells were infected at MOI 0.1 with VACV L-EGFP in
479 presence of H42, R90 or the MRT compounds. 24h post infection (hpi) cells were quantified by flow
480 cytometry for EGFP and displayed as normalised to infected + DMSO (black lines). Cytotoxicity was
481 assessed using a WST-1 assay and displayed as normalised to DMSO (red dashed lines). Data
482 represents biological triplicates and error bars represent the standard deviations of those data.

483

484 **Fig 2. M23, M24, and M25 reduce virus 24h yield and inhibit plaque formation.**

485 A) HeLa cells were infected with WT VACV at MOI 1 in presence of the indicated compounds. At 24
486 hpi cells were harvested and VACV progeny quantified by a titre on BSC40 cells (plaque forming units
487 (pfu)/ml). Data represents biological triplicates and error bars represent the standard deviations of
488 those data. B) A-RPE-19 cells were infected with WT VACV (200 pfu) in the presence of indicated
489 compounds. At 48 hpi cells were subjected to fixation and staining to visualize plaques. Experiments
490 were performed in biological duplicate and representative wells of those experiments are shown.

491

492 **Fig 3. M23, M24 and M25 block LGE and reduce replication site size.**

493 A) HeLa cells were infected with either VACV E-EGFP or VACV L-EGFP at MOI 20 in the presence of
494 the indicated compounds. At 8 hpi cells were harvested and EGFP expressing cells quantified by flow
495 cytometry. Data displayed as normalised to infected + DMSO = 1. Data represents biological
496 triplicates and error bars represent the standard deviations of those data. B) HeLa cells were

497 infected with VACV A5-EGFP (green) at MOI 20 in presence of indicated compounds, concentrations
498 as in A. At 24 hpi fixed cells were immunostained for I3 (magenta), stained with DAPI (blue) and
499 imaged. Scale bar = 20 µm. Experiments were performed in biological duplicate and representative
500 images of those experiments are shown.

501

502 **Fig 4. Inhibitory activity of Bisbenzemides and MRT compounds against Monkeypox virus.**

503 Hft cells in 96-well plates were infected with mpox virus (MOI 0.1) in the presence of 3-fold serial
504 dilutions of TPOXX, H42, M23, M24 or M25. At 48 hpi, virus induced CPE was quantified from fixed
505 and Coomassie-stained plates. Cell viability was quantified from compound-treated, uninfected cells
506 by measuring the conversion of resazurin to fluorescent resofurin. Percentage CPE was normalised
507 to infected and uninfected controls, while percentage cell viability was normalised to untreated cells
508 and high toxicity control (50% DMSO). For both CPE and toxicity measurements, data represents
509 biological triplicates and error bars represent the standard deviations of those data.

510

511 **Fig 5. Bisbenzemides are effective against a TPOXX resistant VACV recombinant.**

512 A) HeLa cells were infected with VACV WT, G277C, or RevG277C viruses at MOI 0.01, to
513 measure virus spread, in the presence of indicated compounds. Cells were harvested 24 hpi
514 and the virus yield determined by plaque assay. Experiments are biological triplicates and
515 error bars represent the standard deviations of those data. B) ARPE-19 cells were infected
516 with 200 pfu of VACV WT, G277C, or RevG277C viruses, in presence of indicated compounds
517 at concentration as in A. At 48 hpi wells were fixed and stained to visualize virus plaques.
518 Experiments were performed in biological duplicate and representative wells shown. C) HeLa
519 cells were infected with G277C or RevG277C virus in presence of DMSO, H42 or M23
520 (concentrations like in A). At 24 hpi cells were fixed and immunostained for I3 and stained

521 with DAPI. Experiments were performed in biological duplicate and representative wells of

522 those experiments are shown. Scale bar = 20 µm.

523

524

525

526

527

528

529

530

531

532

533

534

535

536

537

538

539

540

541 Figure 1

A

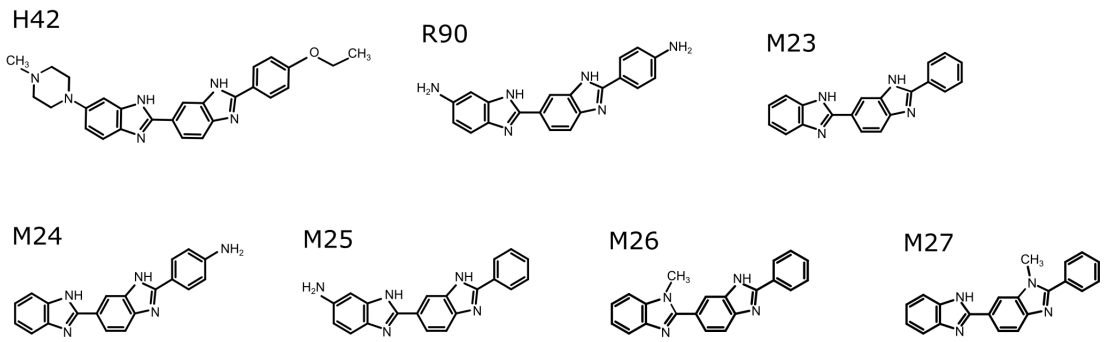

Short Name	H42	R90	M23	M24	M25	M26	M27
LogP	4.75	2.94	4.60	3.77	3.77	4.82	4.82
CAS	23491-52-3	293762-45-5	-	-	-	-	-

B

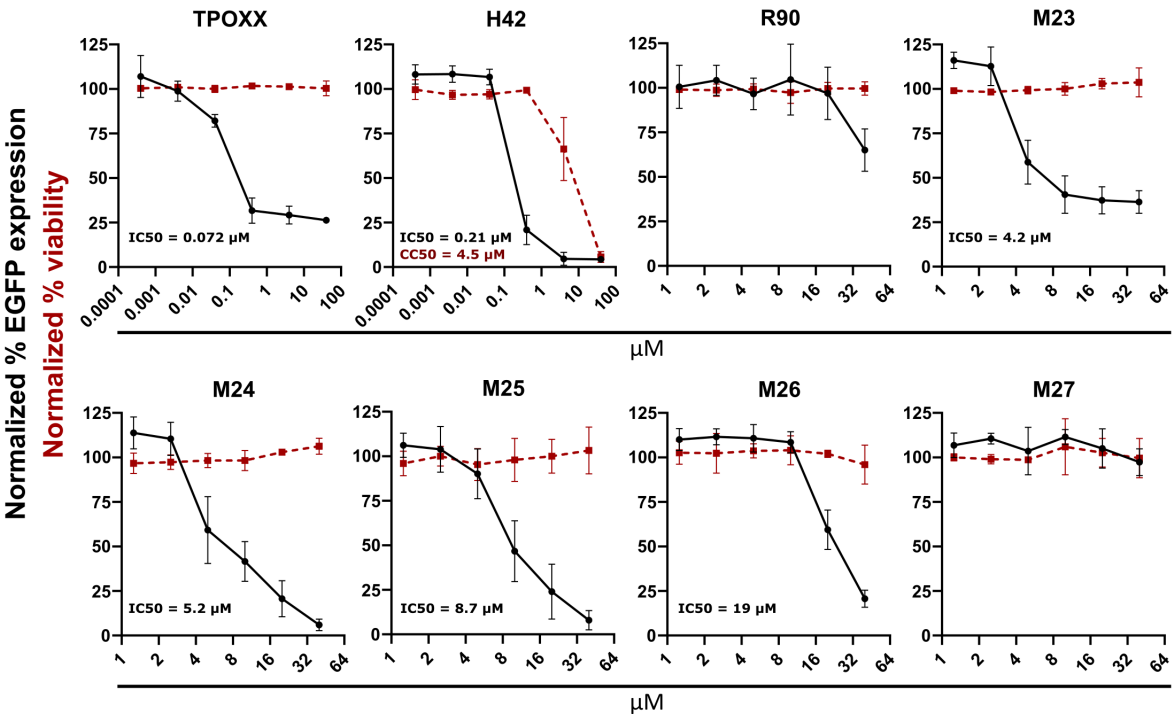

542

543

544

545

546

547 Figure 2

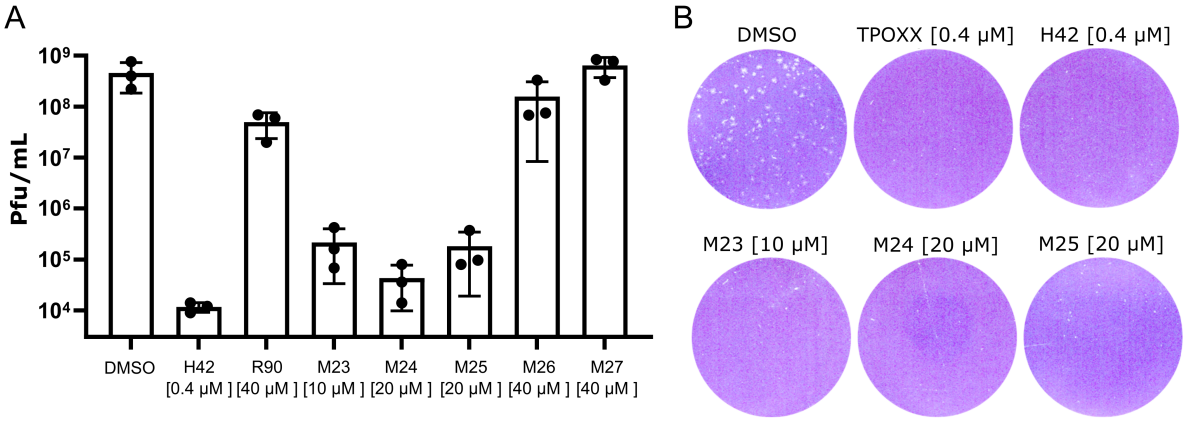

548

549

550

551

552

553

554

555

556

557

558

559

560

561

562

563 Figure 3

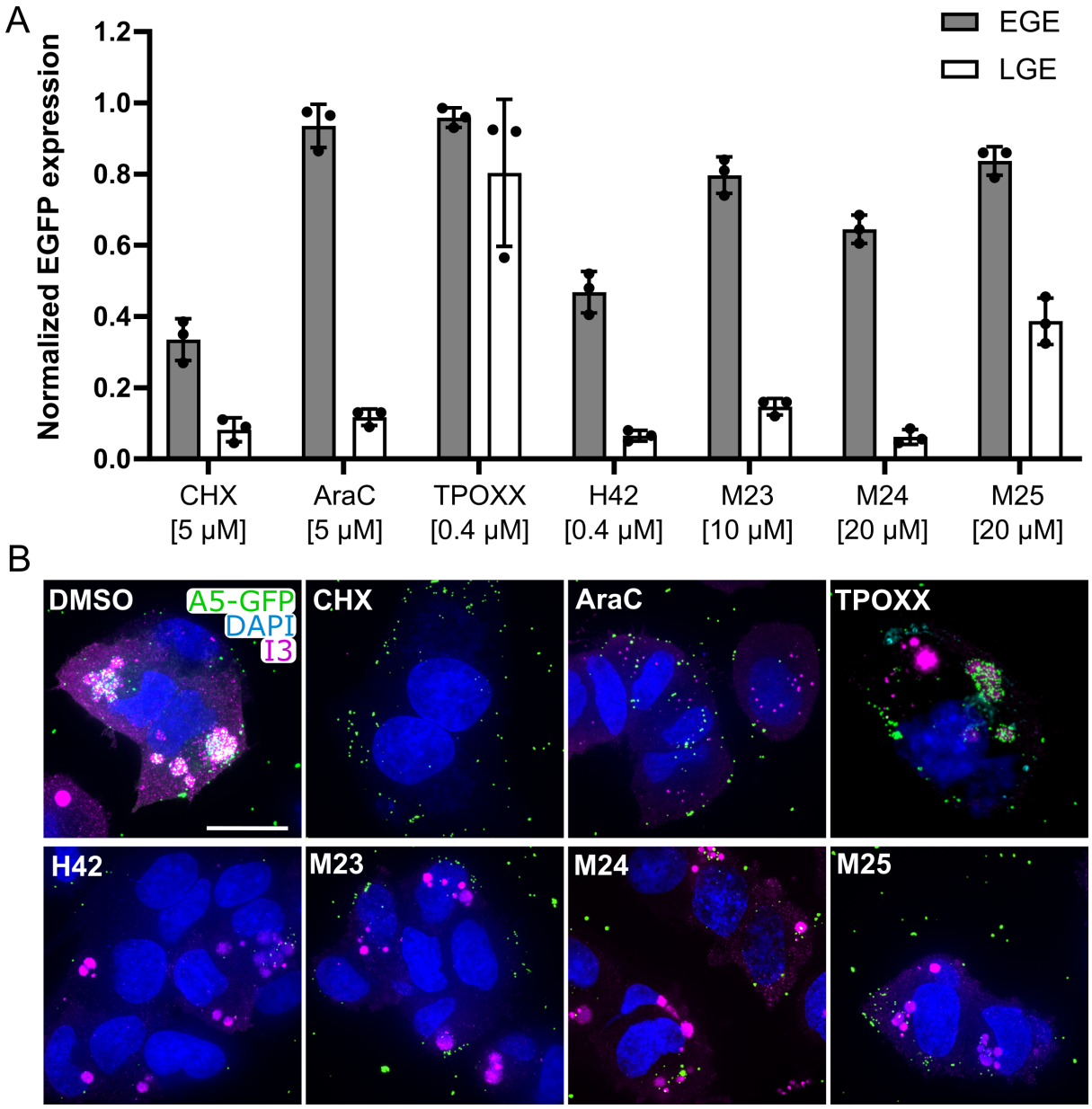

564

565

566

567

568

569

570 Figure 4

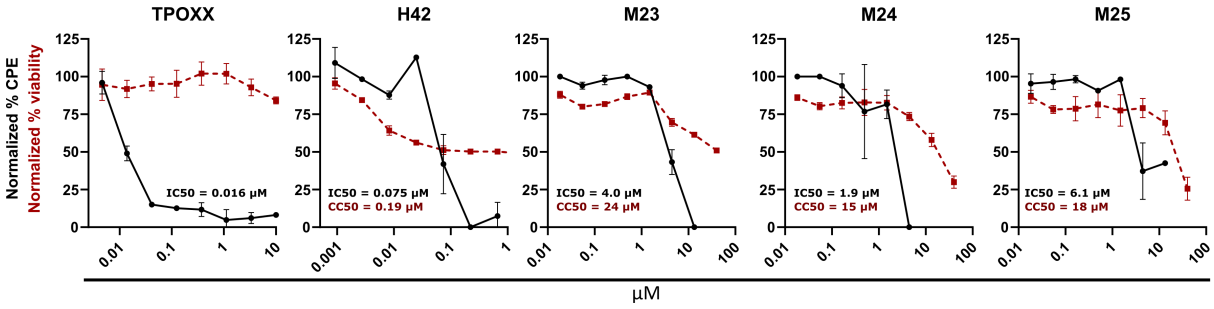

571

572

573

574

575

576

577

578

579

580

581

582

583

584

585

586

587 Figure 5

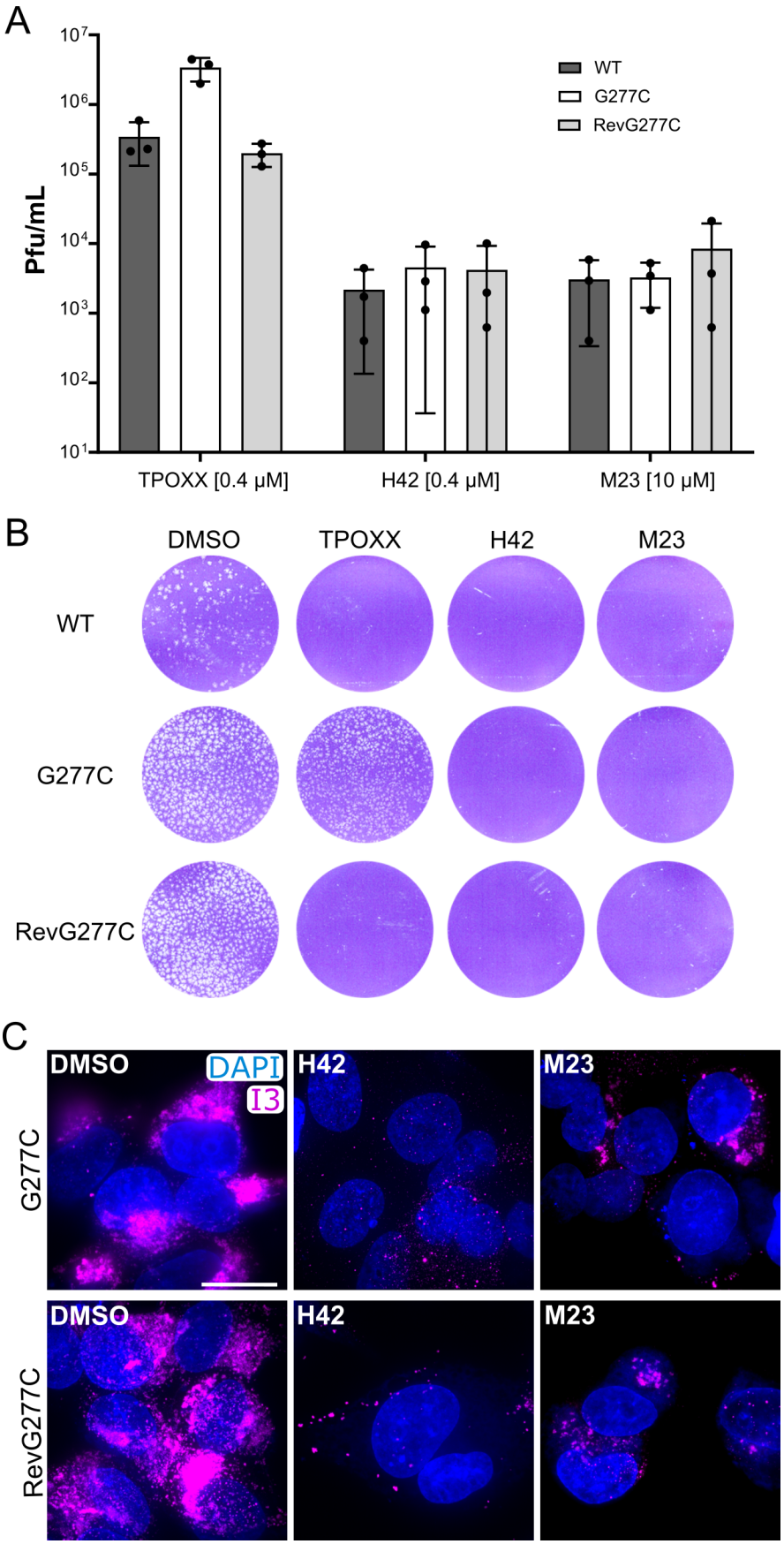

588